Manuscript
Click here to download Manuscript: submitted.doc
Click here to view linked References

University of Utah Institutional Repository
Author Manuscript

UU IR Author Manuscript

UU IR Author Manuscript

Oecologia manuscript number OECO-D-13-00145

Title: Deconvolution of Isotope Signals from Bundles of Multiple Hairs

Christopher H. Remien - Corresponding Author: National Institute for Mathematical and Biological Synthesis, University of Tennessee Knoxville, TN, 37996, Ph. 865-974-4968, cremien@nimbios.org

Frederick R. Adler - Department of Mathematics and Department of Biology, University of Utah, Salt Lake City, UT 84112

Lesley A. Chesson - Department of Biology University of Utah, Salt Lake City, UT 84112, and IsoForensics, Salt Lake City, UT 84108

Luciano O. Valenzuela - Department of Biology University of Utah, Salt Lake City, UT 84112, and IsoForensics, Salt Lake City, UT 84108

James R. Ehleringer - Department of Biology University of Utah, Salt Lake City, UT 84112, and IsoForensics, Salt Lake City, UT 84108

Thure E. Cerling - Department of Geology and Department of Biology, University of Utah, Salt Lake City, UT 84112, and IsoForensics, Salt Lake City, UT 84108 thure.cerling@utah.edu

University of Utah Institutional Repository
Author Manuscript

Abstract

Segmental analysis of hair has been used in diverse fields ranging from forensics to ecology to measure the concentration of substances such as drugs and isotopes. Multiple hairs are typically combined into a bundle for segmental analysis to obtain a high-resolution series of measurements. Individual hair strands cycle through multiple phases of growth and grow at different rates when in the growth phase. Variation in growth of hair strands in a bundle can cause misalignment of substance concentration between hairs, attenuating the primary body signal. We developed a mathematical model based on the known physiology of hair growth to describe the signal averaging caused by bundling multiple hairs for segmental analysis. The model was used to form an inverse method to estimate the primary body signal from measurements of a hair bundle. The inverse method was applied to a previously described stable oxygen isotope chronology from the hair of a murder victim and provides a refined interpretation of the data. Aspects of the reconstruction were confirmed when the victim was later identified.

Keywords: stable isotope, mathematical model, inverse methods

1 Introduction

Organic and inorganic substances in mammals are incorporated into hair, remaining inert for relatively long periods of time [1]. Human forensic applications have long been recognized, as drugs, metabolites, toxins, and poisons are incorporated into hair at the time of formation [2, 3, 4, 5]. More recently, ecologists and anthropologists have used stable isotopes in hair to infer information about an animal's history, including diet, migration, and nutritional status [6, 7, 8, 9, 10, 11]. While the growth of hair is approximately linear, allowing the measurement of long-term chronology through segmental sampling, individual hairs typically have too low linear density to allow high-resolution sampling of a single hair. Sample sizes vary, but segments for drug testing are typically between 10 and 30 mm [2] and generally require 1-300 mg of hair [12]. Stable isotope ratios of hydrogen, carbon, nitrogen,

UU IR Author Manuscript
UU IR Author Manuscript

INSTITUTIONAL REPOSITORY THE UNIVERSITY OF UTAH
University of Utah Institutional Repository
Author Manuscript

oxygen, and sulfur require ca. 200, 50, 300, 200, and 900 μg, respectively. To achieve these masses for animals with hair of relatively low linear density, such as humans, multiple hair strands are typically aligned at the root and combined into a single bundle for analysis [2, 13]. The challenge is to mathematically extract the true chemical signal recorded in hair given variations in growth rate and stasis, because these processes will tend to blur, or average, the temporal information recorded in hair.

Two distinct processes can cause misalignment between individual hair strands in a bundle: variation in growth phase [14] and variation in growth rate [13]. Each hair follicle cycles through three distinct phases of growth [15, 16]. In humans, approximately 90% of hairs are typically in the anagen, or growth, phase, which lasts for 48-72 months. The anagen phase is followed by a brief catagen phase, during which the follicle stops producing hair. The hair then enters the telogen, or resting, phase during which the follicle and hair remain dormant for 2-6 months, until the hair is shed. Variation of growth rate between individual hairs in the growth phase can also blur the measured signal of a hair bundle [13]. The intraindividual coefficient of variation of hair growth in humans is about 0.1 [17, 18], and similar variation has been observed in horses [19] and elephants [20]. Because individual hair strands vary in growth, signal details present in a single hair may not be captured in hair bundle measurements due to averaging misaligned hair strands in a bundle.

Previous studies implicitly assume that the measured bundle signal is equivalent to the signal of a single hair in the growth phase with average growth rate. Given known physiology of hair growth, we assume that the phase of growth and growth rates of individual hairs will vary within a bundle. We have developed a mathematical model of hair growth that describes the relationship between the signal of a bundle of hairs and the primary body signal (e.g., the isotopic pool in the body at equilibrium with hair). The model is based on an estimation of uncertainty in time since formation, or age, of the hair at a given length from the root. We used the model to develop an inverse method to estimate the primary body signal from hair bundle measurements. Our inverse method was applied to a previously described stable oxygen isotope chronology from a hair bundle of a murder victim [21] and provides a refined

UU IR Author Manuscript
UU IR Author Manuscript

INSTITUTIONAL REPOSITORY THE UNIVERSITY OF UTAH
University of Utah Institutional Repository
Author Manuscript

interpretation of the original data.

2 Methods

2.1 Model formulation

2.1.1 Mapping single hair signal to hair bundle measurements

Let $\phi(t)$ be the time-dependent primary body signal (e.g., drug, metabolite, isotope, etc.) to the hair. The function $\phi(t)$ refers to the input signal to the hair (e.g., the isotopic pool in the body at equilibrium with hair), not the input signal to the body (e.g., drinking water, drug dosage history, etc.), and is assumed to be equivalent to the signal of a single hair in the growth phase with the average growth rate. The expected bundle signal as a function of length is

$$\psi(l) = \int \lambda(l,\tau)\phi(\tau)d\tau, \qquad (1)$$

where $\lambda(l,a)$ is the probability density function of time since formation, or age, of a hair at length l from the root given that the total length of the hair is at least l and the hair has not yet been shed. The kernel λ quantifies the length-dependent uncertainty in age.

2.1.2 Evaluation of $\lambda(l,a)$

Let $\lambda(l,a)$ be the probability density function for the random variable time since formation, or age, A, of hair at length l from the root, given that the hair has not been shed and the total length of the hair is at least l. We assume that hair grows at constant random rate R for random time S, and then rests for random time T. We found the distribution of λ in terms of the probability distributions of R, S, and T denoted in Tab. 1 to be

$$\lambda(l,a) = g(l)\frac{l}{a^2}h\left(\frac{l}{a}\right) + \left(1-g\left(l\right)\right)\int_0^a \frac{l}{(a-\tau)^2}\kappa(\tau)h\left(\frac{l}{a-\tau}\right)d\tau$$

where

UU IR Author Manuscript
UU IR Author Manuscript

INSTITUTIONAL REPOSITORY THE UNIVERSITY OF UTAH
University of Utah Institutional Repository
Author Manuscript

$$g(l) = \int_0^\infty h(r) \int_{l/r}^\infty \int_{l/r}^{v} \frac{s - l/r}{v - l/r} f_S(s) f_T(v - s) \, ds \, dv \, dr$$

and

$$\kappa(a) = \int_a^\infty \frac{f_T(x)}{x} dx$$

Refer to the Electronic Supplemental Material for a complete derivation.

2.1.3 Averaging due to sample interval

Signal attenuation also occurs by combining material over the sample length to obtain the mass of material required for analysis. In the case of sampling a single hair that is in the growth phase with fixed growth rate *r*, the expected measured signal, $f(l)$, is the average of the time-dependent primary body signal, $\phi(t)$, converted to length, over the sample length v:

$$f(l) = \frac{r}{v} \int_{l/r - v/(2r)}^{l/r + v/(2r)} \phi(\tau) \, d\tau \, .$$

The center of the samples are at lengths $l = (2i - 1)v/2$ where *i* is a positive integer. Sampling a bundle containing a large number of hairs allows for small sample length, so the measured signal of a bundle of hairs approaches $\psi(l)$.

2.2 Inverse method

To estimate the time-dependent input signal $\phi(t)$ from measurements of $\psi(l)$, we discretized equation 1 into the matrix vector equation $Kf = d$, where f is a discretization of $\phi(t)$, d is a vector containing the measured values of $\psi(l)$, and *K* is an *m*x*n* matrix. The discretization of $\phi(t)$ was chosen to have the same step size as the measurements *d*.

As in the estimation of a primary input signal from a measured stable isotope tooth enamel

UU IR Author Manuscript
UU IR Author Manuscript

INSTITUTIONAL REPOSITORY THE UNIVERSITY OF UTAH
University of Utah Institutional Repository
Author Manuscript

signal described by Passey et al. [22], we used Tikhonov regularization to invert *K*, yielding the estimation $f_{est} = f_{guess} + K^T \left[KK^T + \varepsilon^2 I \right]^{-1} \left[d - Kf_{guess} \right]$, where *I* is an identity matrix, f_{guess} is an *a priori* reference vector, and ε is a scalar regularization parameter. The reference vector f_{guess} was chosen to be a vector containing the mean value of the measurements *d*.

The damping factor ε was chosen using generalized cross-validation. The chosen ε minimizes the GCV functional $GCV(\varepsilon) = \dfrac{\frac{1}{n}\|r_\varepsilon\|^2}{\left[\frac{1}{n} trace(I - A_\varepsilon)\right]^2}$, where $r_\varepsilon = Kf_{est} - d$ and $A_\varepsilon = K\left(K^T K + \varepsilon^2 I\right)^{-1} K^T$ [23].

3 Results

Using the distributions in Tab. 2, the model depends on two parameters: γ is the fraction of hairs in the resting phase (catagen and telogen), and α is the coefficient of variation of hair growth rate. The integral transform kernel, $\lambda(l,a)$, is the probability density function of time since formation, or age, of hair at a given length from the root and describes the amount of signal attenuation in the hair bundle signal. Using the distributions in Tab. 2, the kernel $\lambda(l,a)$, with $\gamma = 0.1$ and $\alpha = 0.1$, is shown in Fig. 1. We varied γ and α to assess how these parameters affect $\lambda(l,a)$ (Fig. 2). A high fraction of hairs in the resting phase, γ, results in high variance in age of hair at all lengths and a mean age that is higher than the length divided by the mean growth rate. A high coefficient of variation of hair growth rate, α, results in increasing variance of age with length. The distribution of age dictates the uncertainty in time when sampling a single hair and also the expected amount of averaging from sampling a bundle of multiple hairs.

The assumed stable isotope primary input signals in Fig. 3 and Fig. 4 are from single elephant tail hairs sampled at 5 mm intervals. Elephants have thick hairs with high linear density, allowing for

UU IR Author Manuscript
UU IR Author Manuscript

INSTITUTIONAL REPOSITORY THE UNIVERSITY OF UTAH
University of Utah Institutional Repository
Author Manuscript

high-resolution sampling of a single hair. The data in Fig. 3 represent an individual migrating between two areas with different $\delta^{15}N$ values for vegetation and thus an abrupt change in hair $\delta^{15}N$ occurs at each migration event [24]; transitions between areas were made in less than 12 hours based on GPS-tracking data. Migration events result in a signal approximating a step function. Data from this individual are previously unpublished, but the individual had behavior analogous to that described by Cerling et al. [24]. We extended this signal periodically to create a longer signal. The data in Fig. 4 are from Cerling et al. [9] and represents gradual diet transitions coinciding with two rainy seasons per year.

We compared the expected value of the signal from sampling a bundle of hairs that contains hairs with varying growth rates and phases, with $\gamma = 0.1$ and $\alpha = 0.1$, to sampling a single hair that has a growth rate of 1 cm/month and sample length $\nu = 1.5$ cm (Fig. 3). The primary body signal refers to the signal of the body pool at equilibrium with hair and is the signal of a single hair in the growth phase with average growth rate. Signal attenuation occurs when sampling a single hair because of combining material over the sample length. Combining multiple hairs into a bundle for sampling attenuates the primary body signal because of varying growth phases and growth rates of hairs in the bundle. Signal details of sufficiently short duration are highly damped and are not captured in the bundle signal because of averaging. When sampling a single hair, events of duration shorter than the sample length may not be recorded. Additionally, when sampling a single hair there is considerable uncertainty in assigning time to length since the exact growth rate and phase of growth of the sampled hair is not usually known.

To test the ability of the inverse method to accurately reconstruct a primary body signal from measurements, we used the forward hair bundle model, with $\gamma = 0.1$ and $\alpha = 0.1$, to create a synthetic measured bundle signal from an assumed primary body signal. We then used the inverse method to estimate the primary body signal from the synthetic bundle signal (Fig. 4). The estimated primary body

UU IR Author Manuscript
UU IR Author Manuscript

INSTITUTIONAL REPOSITORY THE UNIVERSITY OF UTAH
University of Utah Institutional Repository
Author Manuscript

signal is more similar to the primary body signal (correlation coefficient $r^2 = 0.81$) than the measured hair bundle signal is to the primary body signal (correlation coefficient $r^2 = 0.43$). High frequency details are lost in the estimated input signal, but the general pattern remains well estimated.

4 Application of inverse method to murder victim data

We used Tikhonov regularization to reconstruct the $\delta^{18}O$ primary body signal of an unidentified murder victim from stable isotope measurements of the organic component of a hair bundle, with $\gamma = 0.1$ and $\alpha = 0.1$, (Figs. 5 A and 5 B) [21, 25]. The murder victim, nicknamed by law enforcement "Saltair Sally," was found near Salt Lake City, Utah in October 2000. Oxygen stable isotope measurements of the organic component of hair can be used to determine time-dependent geographic region-of-origin because oxygen isotopes in drinking water vary with location [26] and are incorporated into hair [27, 28].

The confidence interval for the estimated primary body signal was obtained by inverting data with noise added to each measurement, representing uncertainty related to analysis. We created 1000 replicates of measurements by adding normally distributed noise with mean zero and standard deviation of 0.15‰ to each measurement. For each set of measurements with added noise, we selected a regularization parameter using generalized cross validation, and performed the inversion using Tikhonov regularization to estimate the primary body signal. We excluded two estimates of the primary body signal because their isotope values lay outside the biologically feasible range of 5 to 18‰. The shaded region corresponds to $\delta^{18}O$ within two standard deviations of the mean estimated primary body signal. We tested the sensitivity of the inversions to changes in γ and α by increasing and decreasing γ and α by 50% and performing the inversions as above. The amplitude of peaks are most sensitive to α, the coefficient of variation of hair growth (Figs. S3, S4, S5, S6). A high value of α leads to larger amplitude transitions, while a low value of α leads to inversions that are more damped. The

UU IR Author Manuscript
UU IR Author Manuscript

INSTITUTIONAL REPOSITORY THE UNIVERSITY OF UTAH
University of Utah Institutional Repository
Author Manuscript

general pattern, however, is robust to changes in γ and α.

The model inversion yields an estimate of the primary body pool at equilibrium with the hair, not the input signal to the body. The body equilibrium signal refers to the primary body signal if it were in instantaneous equilibrium with the input. The body equilibrium signal can be reconstructed using a previously described method based on multiple pools with first order kinetics contributing to the primary body pool that is at equilibrium with hair [29, 30]. For application to the murder victim data, we used a single pool with half-life of 7 days, which is consistent with observations of hair oxygen stable isotopes in humans (calculated from [27, 28]). In this case, the estimated equilibrium signal is very similar to the estimated primary body signal because of rapid turnover of the primary body pool relative to changes in the input signal (refer to the Electronic Supplemental Material for more detail).

Region-of-origin maps were created in two steps. For each region, we used the semi-mechanistic model by Ehleringer et al. [28] to predict drinking water $\delta^{18}O$ values required to produce the hair isotope ratio, with an added 0.5‰ to either side of the value. Once the maximum and minimum $\delta^{18}O$ values of drinking water were predicted for each isotopic region, we used the $\delta^{18}O$ tap water isoscape produced by Bowen et al. [31] for the contiguous United States to identify regions with isotope values matching our predicted range. Regions with matching isotope values were highlighted in color using ArcGIS 9.3.1 ®.

The data were originally interpreted as movement between three isotopically distinct geographic regions, Regions 1, 2, and 3, corresponding to measured $\delta^{18}O$ values of approximately 9.9‰, 8.4‰, and 9.2‰, respectively [21]. The transitions from Region 1 to Region 2 and from Region 2 to Region 1 at about 20 cm and 15 cm, respectively, occur over multiple cm (or equivalently multiple months) of growth, slow movement between geographic regions. The transitions from Region 1 to Region 3 and from Region 3 to Region 1 at about 9 cm and 5 cm, respectively, occur over a short length 10 interval, rapid movement between geographic regions. Region 1 is consistent with the location where the victim

UU IR Author Manuscript
UU IR Author Manuscript

University of Utah Institutional Repository
Author Manuscript

was found, Salt Lake City, UT.

The estimated equilibrium signal differs from the measured hair bundle in several important ways (Figs. 5 A, 5 B, S1, and S2). Transitions between isotopically distinct regions are more rapid, with more time spent in each region. Region 2* and Region 3* have lower $\delta^{18}O$ than Region 2 and Region 3, respectively, and may correspond to different geographic regions (Fig. S1). Regions 2* and 3* have considerable overlap (Fig. S2), suggesting that they may correspond to the same geographic location. Region 1 is isotopically similar in both the measurements and the estimated equilibrium signal, and the $\delta^{18}O$ is consistent with the location where the victim was found. The estimated equilibrium signal has a new short duration region, Region 4, with $\delta^{18}O$ of about 11‰ that does not appear in the measured hair bundle signal. Plotted maps were restricted to the western United States. Region 4 also contains a small region in the northeast United States as well as parts of Canada.

5 Discussion

Multiple hairs that may be in different growth phases and have different growth rates are typically combined into a single bundle of hairs for segmental analysis. We have developed a mathematical model that describes the signal averaging caused by bundling hairs for analysis as well as an inverse method to estimate the primary body signal from measurements of a hair bundle. If the growth rates of hairs within a bundle vary substantially or a high proportion of hairs are in the resting phase of hair growth, the measured hair bundle signal is highly averaged relative to the primary body signal, which may lead to misinterpretation of the signal.

Our model is based on uncertainty in time since formation, or age, of hair a given length from the root. Assigning times to length when sampling a single hair strand also relies on an estimation of length-dependent age variation. High variation in growth rates or a high proportion of hairs in the resting phase of hair growth leads to high uncertainty in assigning time to measurements along the

UU IR Author Manuscript
UU IR Author Manuscript

INSTITUTIONAL REPOSITORY THE UNIVERSITY OF UTAH
University of Utah Institutional Repository
Author Manuscript

length of a single hair strand.

The determination of whether to bundle hairs or sample a single hair depends on the research question. If precise timing of an event is critical or high-resolution sampling is desired to capture events in the recent past, multiple hairs should be combined into a bundle to decrease sample length and reduce uncertainty in the time corresponding to measurements. If multiple hairs are to be combined, it is preferred to combine many hairs rather than few, as the uncertainty in the bundle signal decreases with the number of hairs. If the amplitude of a long duration event is more important or an individual hair strand has high enough linear density to allow for a high-resolution sample interval, sampling a single hair strand may result in less signal averaging than sampling a bundle of hairs. When sampling a single hair, however, there may be high uncertainty in assigning time to measurements.

The inverse method we developed allows for the estimation of the primary body signal from a measured hair bundle signal. The method is especially useful in situations where the primary body signal is averaged, but characteristics of the signal remain. If the averaging is significant enough, however, noise may dominate, preventing meaningful reconstruction of the primary body signal.

It may be possible to minimize signal averaging from bundling multiple hairs by ensuring hairs are in the growth phase. Van Scott et al. have described a technique to examine a hair's follicle to determine its phase of growth [32], though this is only possible if a hair's root can be observed (i.e., hair was plucked rather than cut). Excluding hairs in the resting phase from a bundle has been shown to reduce the growth cycle error in hair stable isotope analysis [33]. This can be incorporated into our model by reducing γ, the fraction of hairs in the resting phase, which results in less signal averaging. If the hair has never been cut, selecting hairs for analysis with small total length also increases the likelihood of hair being in the growth phase. Since each hair grows for a period of time before shedding, hairs with small total length are more likely to be in the growth phase. However, the bundled signal will still be attenuated due to variation in growth rate of individual hairs.

We applied our inverse method to a previously described [21, 25] oxygen stable isotope

UU IR Author Manuscript
UU IR Author Manuscript

INSTITUTIONAL REPOSITORY THE UNIVERSITY OF UTAH
University of Utah Institutional Repository
Author Manuscript

chronology from the organic component of the hair of a murder victim. The signal obtained from the inverse method is an estimate of the $\delta^{18}O$ of the primary body pool that is in equilibrium with the hair, rather than the time-dependent isotopic composition of drinking water. Applying a model of turnover of the primary body pool $\delta^{18}O$ to the estimated primary body signal provides an estimate of the equilibrium signal. This further sharpens the transitions between regions, though the effect is small due to the relatively rapid turnover of oxygen isotopes in the primary body pool at equilibrium with hair. In cases where turnover of the body pools at equilibrium with hair is slow (e.g., carbon [34] and nitrogen isotopes [35]), the signal attenuation caused by turnover of the body pools may be larger than that caused by bundling multiple hairs. The search maps determined by the estimated equilibrium signal differ from previously published interpretations in several important ways. Transitions between isotopically distinct regions are more rapid, and predicted regions have slightly different $\delta^{18}O$. An additional region of short duration with relatively high $\delta^{18}O$ is present in the estimated equilibrium, that may have been averaged by measuring a bundle of multiple hairs.

The murder victim has since been identified through DNA analysis as Nikole Bakoles. There are several insights and consistencies between model predictions and observations from Nikole's life. Nikole was a known traveler, and the hair record shows this. Nikole is known to have spent time with her parents, and this shows up in the Seattle-Tacoma predictions. She was a resident of Salt Lake County, who moved in and out of the area, and this shows up in the isotope record of her hair. A major unknown is that the model predicts a third area, north of Salt Lake City. At the moment, investigators do not know about these travels.

In some animals, hair grows seasonally. If the growth phases of individual hair strands are correlated, the signal of a hair bundle will have lower attenuation relative to the primary body signal because hairs are likely to be in the same growth phase. There will, however, still be variation in hair growth rate between hairs, and variation in hair growth rate between hairs may have a larger effect on

UU IR Author Manuscript
UU IR Author Manuscript

University of Utah Institutional Repository
Author Manuscript

attenuating the signal (Supplemental Figures S1, S2, S3, and S4).

Similar methods may also be used to estimate uncertainty in time since formation, when time cannot be constrained using other methods, in other length-dependent measurements of ecological tape recorders, such as measurements of nails, horn, or tropical trees lacking growth rings. Additionally, similar probability density functions may be useful for estimating the uncertainty in age of an animal or plant from size or length. The details of these methods will depend on growth characteristics. Other biological systems, such as cell-cycle dependent processes, also rely on inverse methods to estimate individual signal from population-level measurements [36, 37, 38, 39]. In these models, variation in cell-cycle phase of individual cells can result in important differences between population measurements and individual cell dynamics.

Hair records the concentration of drugs, toxins, metabolites, and stable isotopes in the body as it grows. Segmental analysis of a bundle of hair allows for the construction of a high-resolution record of the history of an animal. However, variation in the growth of individual hair strands can distort the relation between measurements and the actual history of the animal. Our mathematical model provides an estimate of uncertainty in time since formation, or age, of a hair strand a given length from the root as well as an inverse method to estimate the time-dependent primary body signal (e.g., drug, metabolite, isotope, etc.) from segmental analysis of a bundle of hairs, based on measurable growth characteristics of individual hair strands.

6 Acknowledgments

CHR conducted this work as a University of Utah Research Training Group Fellow through NSF award #EMSW21-RTG and as a Postdoctoral Fellow at the National Institute for Mathematical and Biological Synthesis, an Institute sponsored by the National Science Foundation, the U.S. Department of Homeland Security, and the U.S. Department of Agriculture through NSF Award #EF-0832858, with additional support from The University of Tennessee, Knoxville.

UU IR Author Manuscript
UU IR Author Manuscript

INSTITUTIONAL REPOSITORY THE UNIVERSITY OF UTAH
University of Utah Institutional Repository
Author Manuscript

References

[1] Henderson GL. Mechanisms of drug incorporation into hair. Forensic Science International, 63:19-29, 1993.

[2] Cooper GAA, Kronstrand R, and Kintz P. Society of Hair Testing guidelines for drug testing in hair. Forensic Science International, 2011.

[3] Sachs H. History of hair analysis. Forensic Science International, 84:7-16, 1997.

[4] Selavka CM and Rieders F. The determination of cocaine in hair: A review. Forensic Science International, 70:155-164, 1995.

[5] Staub C. Analytical procedures for determination of opiates in hair: A review. Forensic Science International, 70:111-123, 1995.

[6] Martinez del Rio C, Wolf N, Carleton SA, and Gannes LZ. Isotopic ecology ten years after a call for more laboratory experiments. Biological Reviews, 84:91-111, 2009.

[7] Crawford K, McDonald RA, and Bearhop S. Applications of stable isotope techniques to the ecology of mammals. Mammal Review, 38(1):87-107, 2008.

[8] Wolf N, Carleton SA, and Martinez del Rio C. Ten years of experimental animal isotopic ecology. Functional Ecology, 23(1):17-26, 2009.

[9] Cerling TE, Wittemyer G, Ehleringer JR, Remien CH, and Douglas-Hamilton I. History of animals using isotope records (HAIR): A 6-year dietary history of one family of African elephants. Proc Nat Acad Sciences (USA), 106:8093-8100, 2009.

[10] Petzke KJ, Fuller BT, and Metges CC. Advances in natural stable isotope ratio analysis of human hair to determine nutritional and metabolic status. Current Opinion in Clinical Nutrition and Metabolic Care, 13(5):532-540, 2010.

[11] Schwertl M, Auerswald K, and Schnyder H. Reconstruction of the isotopic history of animal diets by hair segmental analysis. Rapid Communications in Mass Spectrometry, 17:1312-1318, 2003.

UU IR Author Manuscript
UU IR Author Manuscript

INSTITUTIONAL REPOSITORY THE UNIVERSITY OF UTAH
University of Utah Institutional Repository
Author Manuscript

[12] Wainhaus SB, Tzanani N, Dagan S, Miller ML, and Amirav A. Fast analysis of drugs in a single hair. J Am Soc Mass Spectrom, 9:1311-1320, 1998.

[13] Lebeau MA, Montgomery MA, and Brewer JD. The role of variations in growth rate and sample collection on interpreting results of segmental analyses of hair. Forensic Science International, 210:110-116, 2011.

[14] Sachs H. Theoretical limits of the evaluation of drug concentrations in hair due to irregular hair growth. Forensic Science International, 70:53-61, 1995.

[15] Chase HB. Growth of the hair. Physiol Rev, 34:113-126, 1954.

[16] Kligman AM. The human hair cycle. J Invest Dermatol, 33:307-316, 1959.

[17] Myers RJ and Hamilton JB. Regeneration and rate of growth of hairs in man. Annals of the New York Academy of Sciences, 53:562-568, 1951.

[18] Lee SH, Kwon OS, Oh JK, Park WS, Moon SE, and Eun HC. Bleaching phototrichogram: an improved method for hair growth assessment. J Dermatol, 32(10):782-787, 2005.

[19] West AG, Ayliffe LK, Cerling TE, Robinson TF, Karren B, Dearing MD, and Ehleringer JR. Short term diet changes revealed using stable carbon isotopes in horse tail-hair. Functional Ecology, 18:616-624, 2004.

[20] Wittemyer G, Cerling TE, and Douglas-Hamilton I. Establishing chronologies from isotopic profiles in serially collected animal tissues: An example using tail hairs from African elephants. Chemical Geology, 263:3-11, 2009.

[21] Ehleringer JR, Thompson AH, Podlesak DW, Bowen GJ, Chesson LA, Cerling TE, Park T, Dostie P, and Schwarcz H. A framework for the incorporation of isotopes and isoscapes in geospatial forensic investigations. In West JB et al., editor, Isoscapes: Understanding movement, pattern, and process on earth through isotope mapping, chapter 17, pages 357-387. Springer, 2010.

[22] Passey BH, Cerling TE, Schuster GT, Robinson TF, Roeder BL, and Krueger SK. Inverse methods for estimating primary input signals from time-averaged intra-tooth isotope profiles. Geochim

UU IR Author Manuscript
UU IR Author Manuscript

INSTITUTIONAL REPOSITORY THE UNIVERSITY OF UTAH
University of Utah Institutional Repository
Author Manuscript

362 Cosmochim Acta, 69:4101-4116, 2005.

363 [23] Vogel CR. Computational Methods for Inverse Problems. SIAM, 2002.

364 [24] Cerling TE, Wittemyer G, Rasmussen HB, Vollrath F, Cerling CE, Robinson TJ, and Douglas-
365 Hamilton I. Stable isotopes in elephant hair document migration patterns and diet changes. Proc Nat
366 Acad Sciences (USA), 103(2):371-373, 2006. 16

367 [25] Kennedy CD, Bowen GJ, and Ehleringer JR. Temporal variation of oxygen isotope ratios ($\delta^{18}O$)
368 in drinking water: Implications for specifying location of origin with human scalp hair. Forensic
369 Science International, 208:156-166, 2011.

370 [26] Bowen GJ and Wilkinson B. Spatial distribution of $\delta^{18}O$ in meteoric precipitation. Geology,
371 30(4):315-318, 2002.

372 [27] O'Brien DM andWooller MJ. Tracking human travel using stable oxygen and hydrogen isotope
373 analyses of hair and urine. Rapid Communications in Mass Spectrometry, 21(15):2422-2430, 2007.

374 [28] Ehleringer JR, Bowen GJ, Chesson LA, West AG, Podlesak DW, and Cerling TE. Hydrogen and
375 oxygen isotope ratios in human hair are related to geography. Proc Nat Acad Sciences (USA),
376 105(8):2788-2793, 2008.

377 [29] Cerling TE, Passey BH, Ayliffe LK, Cook CS, Ehleringer JR, Harris JM, Dhidha MB, and Kasiki
378 SM. Orphans' tales: Seasonal dietarry changes in elephants from Tsavo National Park, Kenya.
379 Palaeogeogr Palaeoclim Palaeoecol, 206:367-376, 2004.

380 [30] Cerling TE, Ayliffe LK, Dearing MD, Ehleringer JR, Passey BH, Podlesak DW, Torregrossa AM,
381 and West AG. Determining biological tissue turnover using stable isotopes: The reaction progress
382 variable. Oecologia, 151:175-189, 2007.

383 [31] Bowen GJ, Ehleringer JR, Chesson LA, Stange E, and Cerling TE. Stable isotope ratios of tap
384 water in the contiguous United States. Water Resour Res, 43:1-12, 2007.

385 [32] Van Scott EJ, Reinertson RP, and Steinmuller RJ. The growing hair root of the human scalp and

UU IR Author Manuscript
UU IR Author Manuscript

INSTITUTIONAL REPOSITORY THE UNIVERSITY OF UTAH
University of Utah Institutional Repository
Author Manuscript

morphological changes therein following ametropin therapy. J Invest Dermatol, 29:197- 204, 1957.

[33] Williams LJ, White CD, and Longstaffe FJ. Improving stable isotopic interpretations made from human hair through reduction of growth cycle error. American Journal of Physical Anthropology, 145:125-136, 2011.

[34] Ayliffe LK, Cerling TE, Robinson T, West AG, Sponheimer M, Passey BH, Roeder B, Dearing MD, and Ehleringer JR. Turnover of carbon isotopes in tail hair and breath CO2 of horses fed an isotopically varied diet. Oecologia, 151:175-189, 2007.

[35] Sponheimer M, Robinson T, Ayliffe L, Roeder B, Hammer J, Passey B, West A, Cerling T, Dearing D, and Ehleringer J. Nitrogen isotopes in mammalian herbivores: Hair $\delta^{15}N$ values from a controlled feeding study. International Journal of Osteoarchaeology, 13:80-87, 2003.

[36] Lu P, Nakorchevskiy A, and Marcotte E. Expression deconvolution: A reinterpretation of DNA microarray data reveals dynamic changes in cell populations. Proc Nat Acad Sciences (USA), 100:10370-10375, 2003.

[37] Bar-Joseph Z, Farkash S, Gifford DK, Simon I, and Rosenfield R. Deconvolving cell cycle expression data with complementary information. Bioinformatics, 20:23-30, 2004.

[38] Rowicka M, Kudlicki A, Tu BP, and Otwinowski Z. High-resolution timing of cell cycle- regulated gene expression. Proc Nat Acad Sciences (USA), 104:16892-16897, 2007.

[39] Siegal-Gaskins D, Ash JN, and Crosson S. Model-based deconvolution of cell cycle time- series data reveals gene expression details at high resolution. PLoS Computational Biology, 5(8):e1000460, 2009.

UU IR Author Manuscript

UU IR Author Manuscript

University of Utah Institutional Repository
Author Manuscript

411

412

413

414

415 Figure Legends
416
417 Figure 1: The kernel $\lambda(l,a)$ at lengths 2.5 cm, 5 cm, 10 cm, and 20 cm, A-D, respectively, describes
418 the variation of time since formation, or age, at a given length from the root.
419
420 Figure 2: Mean, A, and standard deviation, B, of time since formation, or age, of hair at a given length
421 from the root for various values of fraction of hairs in the resting phase, γ, and coefficient of variation
422 of hair growth rate, α.
423
424 Figure 3: Expected length-dependent single hair signal and hair bundle signal derived from our
425 mathematical model using an assumed time-dependent primary body signal. Time indicates months
426 prior to formation of hair at root, length indicates cm from root. The signal of the measured bundle of
427 hairs is highly attenuated relative to the primary body signal.
428
429 Figure 4: A primary body signal that is attenuated from sampling a bundle of hairs can be partially
430 reconstructed from measurements using inverse methods. Time indicates months prior to formation of
431 hair at root, length indicates cm from root.
432
433 Figure 5 A: Estimated primary body signal and equilibrium signal from hair $\delta^{18}O$ measurements of a
434 previously described hair bundle of a murder victim [25, 21]. B: Tap water maps for geographic regions
435 predicted by the estimated equilibrium signal.
436

UU IR Author Manuscript

UU IR Author Manuscript

Table 1
Click here to download Table: table1.doc

University of Utah Institutional Repository
Author Manuscript

Table 1: Definitions of distributions used in modeling.

Distribution	**Description**
h	Probability distribution function for the growth rate of hair, R
H	Cumulative distribution function for the growth rate of hair, R
f_S	Probability distribution function for the time spent in growth phase, S
F_S	Cumulative distribution function for the time spent in growth phase, S
f_T	Probability distribution function for the time spent in resting phase, T
F_T	Cumulative distribution function for the time spent in resting phase, T

UU IR Author Manuscript

UU IR Author Manuscript

Table 2
Click here to download Table: table2.doc

University of Utah Institutional Repository
Author Manuscript

Table 2: Parameters and distributions used in modeling

Parameter	**Description**	**Value**
γ	Fraction of hairs in resting phase	0.05, 0.1, 0.3
α	Coefficient of variation of hair growth rate	0.05, 0.1, 0.25
β	Mean hair growth rate	1 cm/month [17, 13]
ν	Mean time from beginning of growth phase to hair shedding	66 months [14]
Distribution	**Description**	**Value**
h	Hair growth rate probability density function	$N\left(\beta,(\beta\alpha)^2\right)$
f_S	Time in growth phase probability density function	$N\left(\nu(1-\gamma),\left(0.1\nu(1-\gamma)\right)^2\right)$
f_T	Time in resting phase probability density function	$N\left(\nu\gamma,(0.1\nu\gamma)^2\right)$

UU IR Author Manuscript

UU IR Author Manuscript

Figure 1

Click here to download Figure: 031114fig1.pdf

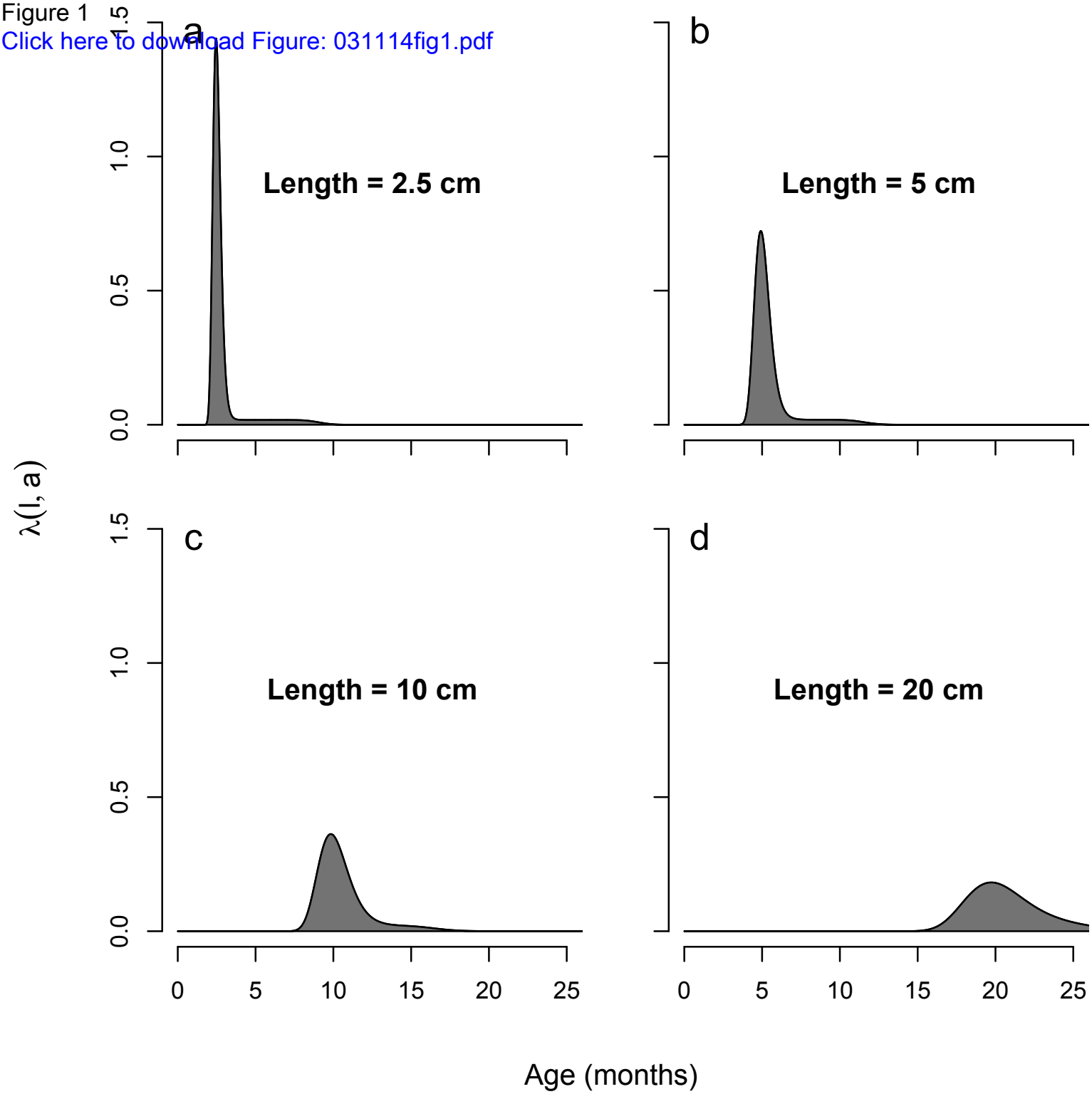

Figure 2

Click here to download Figure: 031114fig2.pdf

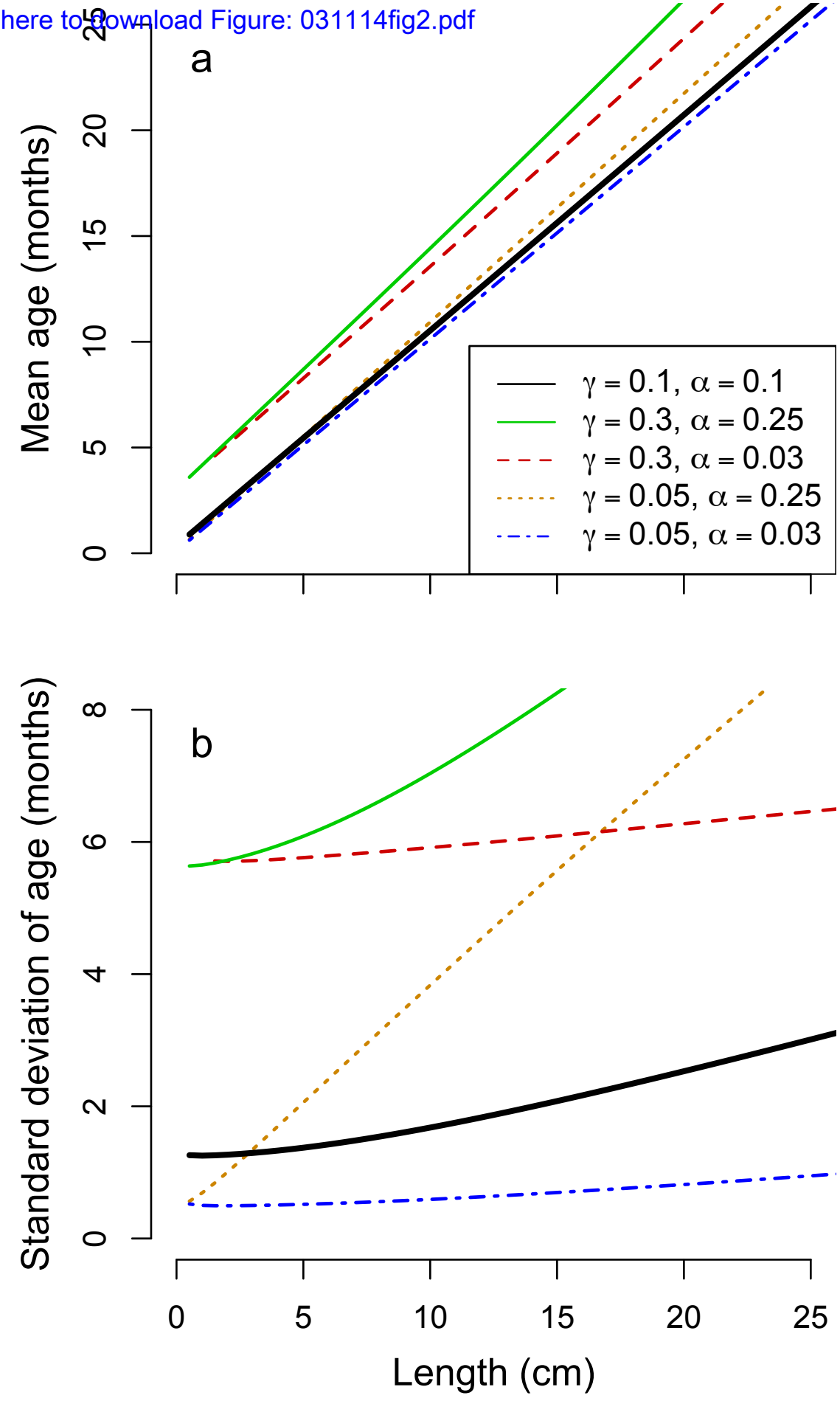

Figure 3

Click here to download Figure: 031114fig3.pdf

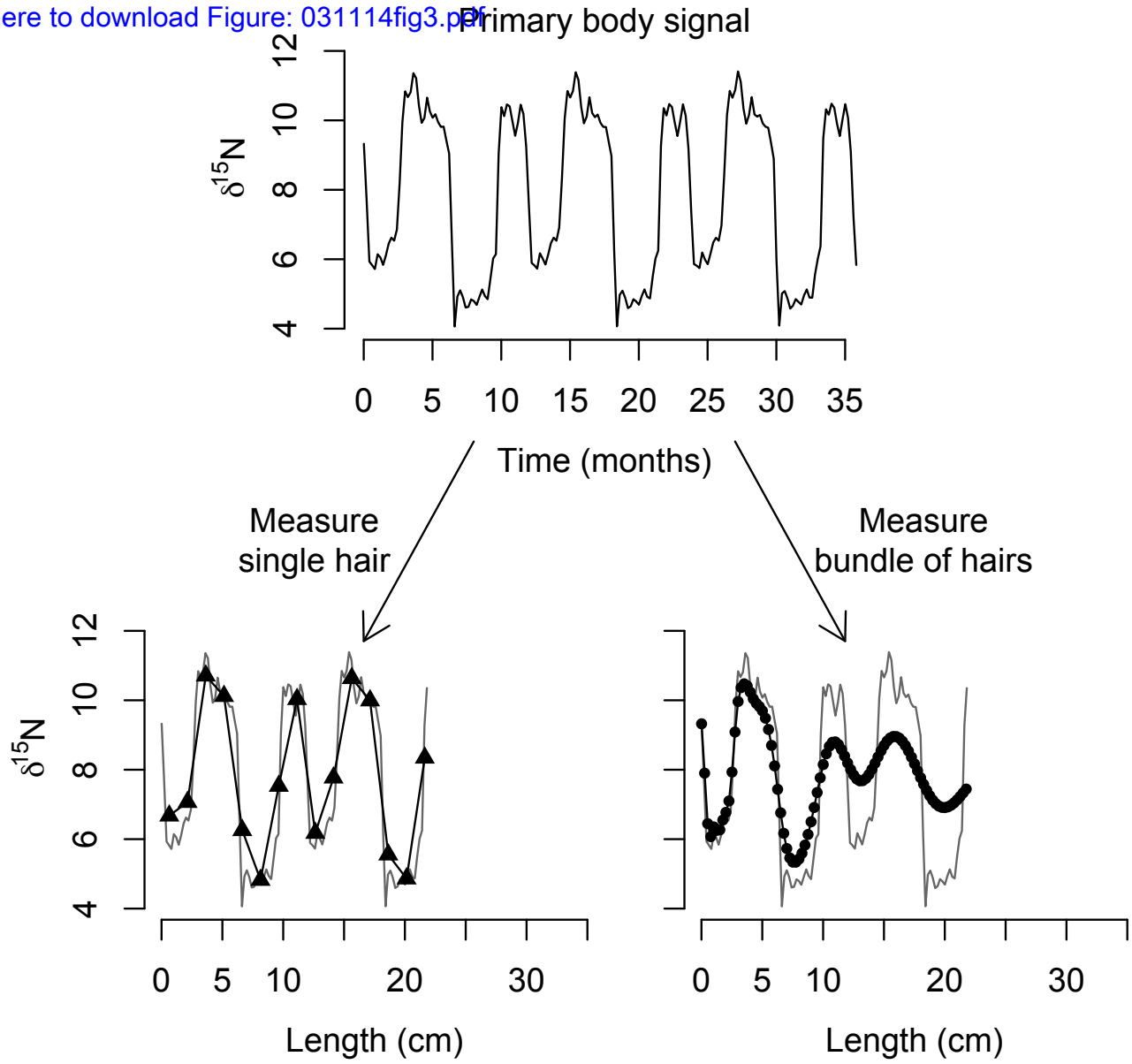

Figure 4

Click here to download Figure: 031114fig4.pdf

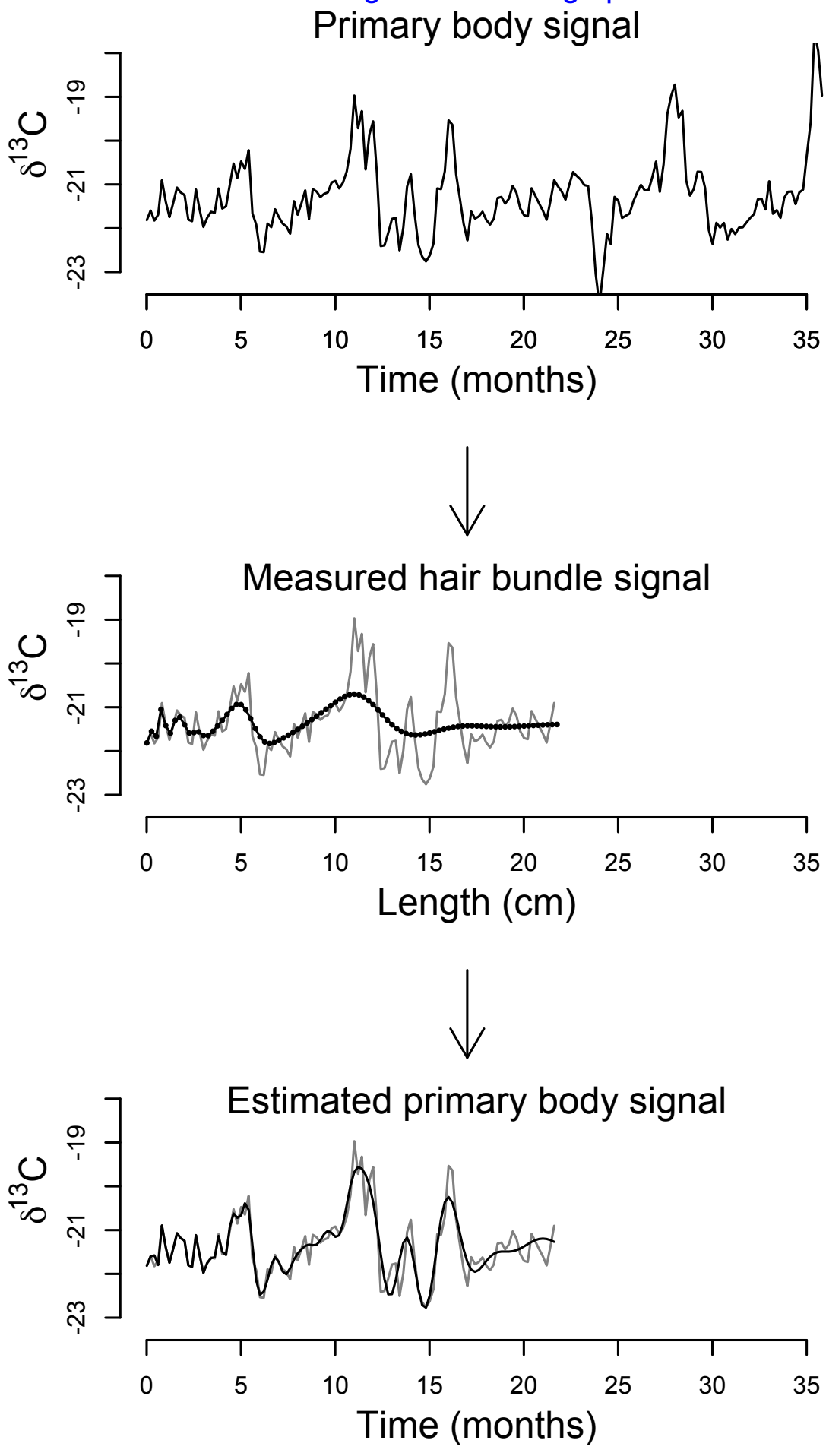

Figure 5a

Click here to download Figure: 031114fig5a.pdf

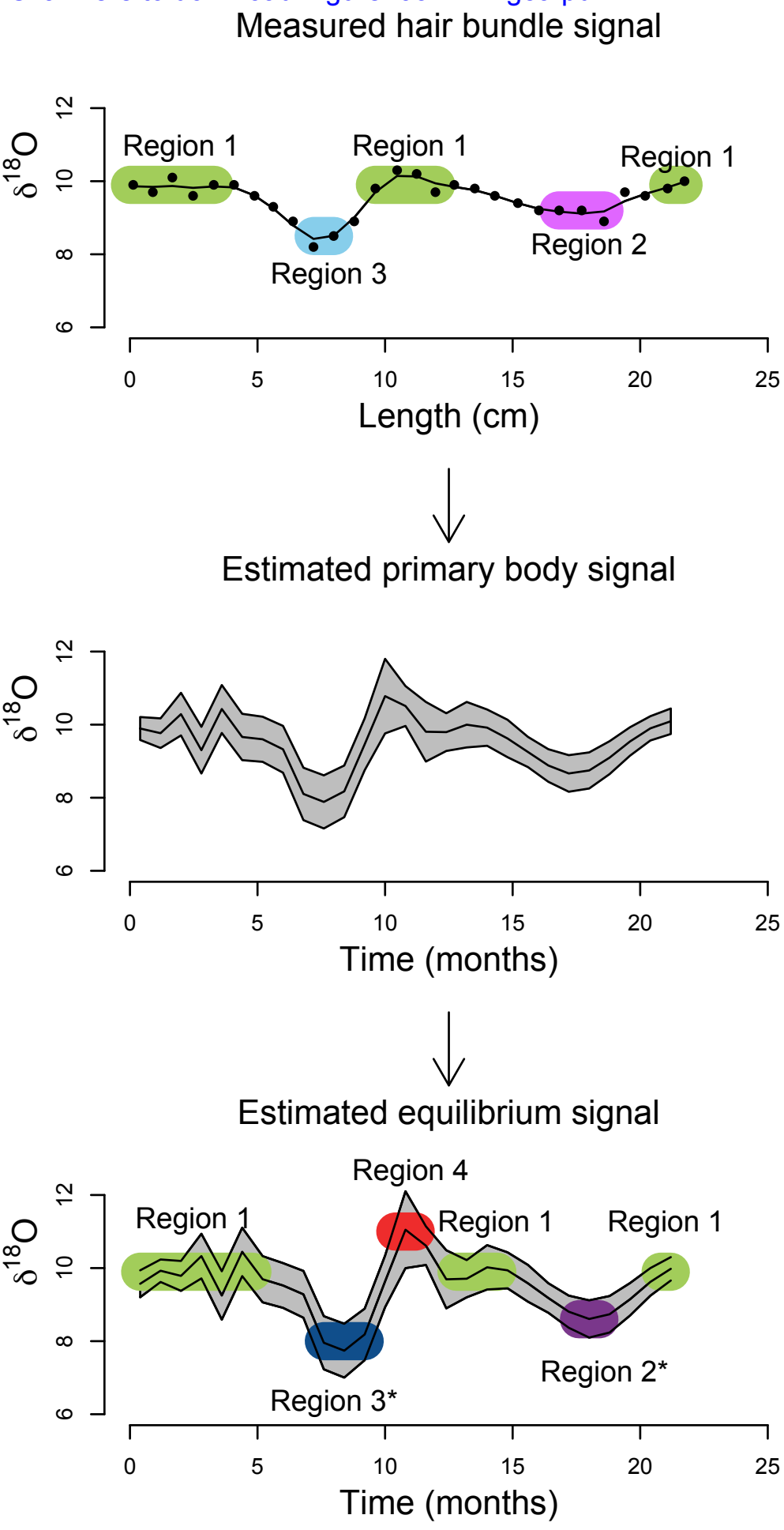

Figure 5b
Click here to download high resolution image

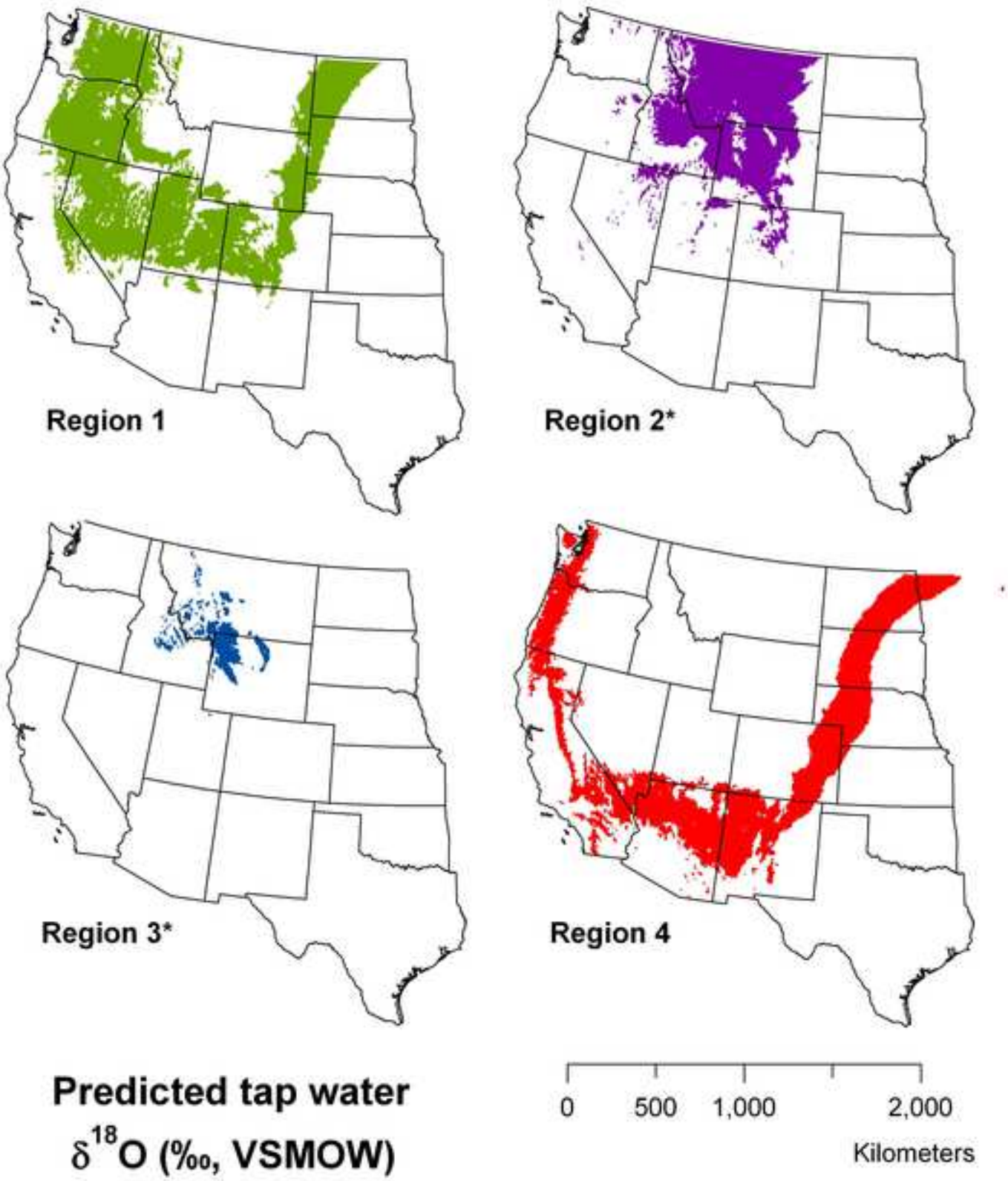

Supplementary Material
Click here to download Supplementary Material: esm.pdf
University of Utah Institutional Repository
Author Manuscript

1 Electronic Supplemental Material

1.1 Derivation of $\lambda(l, a)$

Let $\lambda(l, a)$ be the probability density function for the random variable time since formation, or age, A, of hair at length l from the root, given that the hair has not been shed and the total length of the hair is at least l. Let $\Lambda(l, a)$ be the cumulative distribution function of A, so that $\lambda(l, a) = \frac{d}{da}\Lambda(l, a)$. We assume that hair grows at constant random rate R for random time S, and then rests for random time T. We will find the distribution of Λ in terms of the probability distributions of R, S, and T denoted in Tab. 1.

Let L be the random variable describing the total length of the hair. A hair strand is shed at random time $S + T$. Using the law of total probability, we condition on the phase of growth of the hair.

$$\begin{aligned}\Lambda(l, a) &= \Pr\left(A \leq a | L \geq l \text{ and } A \leq S + T\right) \\ &= \Pr(A \leq a | L \geq l \text{ and } A \leq S)\Pr(A \leq S | L \geq l \text{ and } A \leq S + T) + \\ &\Pr(A \leq a | L \geq l \text{ and } S \leq A \leq S + T)\Pr(S \leq A \leq S + T | L \geq l \text{ and } A \leq S + T)\end{aligned}$$

Let $g(l) = \Pr(A \leq S | L \geq l \text{ and } A \leq S+T)$. We again use the law of total probability to rewrite $\Lambda(l, a)$, this time conditioning upon the amount of time that a hair has been resting, V, given that it is in the resting phase.

$$\begin{aligned}\Lambda(l, a) &= g(l)\Pr(A \leq a | L \geq l \text{ and } A \leq S) \\ &+ (1 - g(l)) \int_{\tau=0}^{a} \Pr(A \leq a | L \geq l \text{ and } S \leq A \leq S + T \text{ and } V = \tau) \\ &* \Pr(V = \tau | S \leq A \leq S + T) d\tau\end{aligned}$$

We will find each of these distributions in terms of the distributions in Tab. 1.

UU IR Author Manuscript
UU IR Author Manuscript

University of Utah Institutional Repository
Author Manuscript

$$\begin{aligned}
&\Pr(A \le a | L \ge l \text{ and } A \le S) \\
&\quad = \int_0^\infty \Pr(A \le a | L \ge l \text{ and } A \le S) \Pr(R = r) dr \\
&\quad = \int_0^\infty \Pr\left(\frac{l}{r} \le a | L \ge l \text{ and } A \le S\right) h(r) dr \\
&\quad = \int_{l/a}^\infty h(r) dr \\
&\quad = 1 - H\left(\frac{l}{a}\right)
\end{aligned}$$

Similarly,

$$\begin{aligned}
&\Pr(A \le a | L \ge l \text{ and } A \le S + T \text{ and } V = \tau) \\
&\quad = \int_0^\infty \Pr(A(l) \le a | L \ge l \text{ and } A \le S + T \text{ and } V = \tau) \Pr(R = r) dr \\
&\quad = \int_0^\infty \Pr\left(\frac{l}{r} + \tau \le a | L \ge l \text{ and } A \le S + T \text{ and } V = \tau\right) h(r) dr \\
&\quad = \int_{l/(a-\tau)}^\infty h(r) dr \\
&\quad = 1 - H\left(\frac{l}{a - \tau}\right)
\end{aligned}$$

To find $\Pr(V = \tau | S \le A \le S + T)$, we find the cumulative distribution function, and then differentiate. Because the stage of hair growth is well mixed between hairs, the amount of time a hair has been resting given that it is in the resting phase, V, is uniformly distributed from 0 to T.

$$\begin{aligned}
\Pr(V \le \tau | S \le A \le S + T) &= \int_0^\infty \Pr(V \le \tau | S \le A \le S + T \text{ and } T = t) \Pr(T = t) dt \\
&= \int_0^\infty \Pr(V \le \tau | S \le A \le S + T \text{ and } T = t) f_T(t) dt \\
&= \int_0^\tau f_T(t) dt + \int_\tau^\infty \frac{\tau}{t} f_T(t) dt \\
&= F_T(\tau) + \tau \int_\tau^\infty \frac{f_T(t)}{t} dt
\end{aligned}$$

UU IR Author Manuscript
UU IR Author Manuscript

INSTITUTIONAL REPOSITORY
THE UNIVERSITY OF UTAH
University of Utah Institutional Repository
Author Manuscript

So that

$$\Pr(V = \tau | S \leq A \leq S + T) = \int_{\tau}^{\infty} \frac{f_T(t)}{t} dt.$$

Again, because the stage of hair growth is well mixed between hairs,

$$\begin{aligned}
g(l) &= \Pr(A \leq S | L \geq l \text{ and } A \leq S + T) \\
&= \int_0^{\infty} h(r) \int_0^{\infty} \int_0^{\infty} \Pr(A \leq s | L \geq l, A \leq s + t, R = r, S = s, T = t) f_S(s) f_T(t) ds dt dr \\
&= \int_0^{\infty} h(r) \int_0^{\infty} \int_0^{\infty} \Pr(A \leq s | l/r \leq A \leq s + t, R = r, S = s, T = t) f_S(s) f_T(t) ds dt dr \\
&= \int_0^{\infty} h(r) \int_0^{\infty} \int_{l/r}^{s+t} \frac{s - l/r}{s + t - l/r} f_S(s) f_T(t) ds dt dr \\
&= \int_0^{\infty} h(r) \int_{l/r}^{\infty} \int_{l/r}^{v} \frac{s - l/r}{v - l/r} f_S(s) f_T(v - s) ds dv dr
\end{aligned}$$

Putting these distributions together we have

$$\Lambda(l, a) = g(l) \left(1 - H\left(\frac{l}{a}\right)\right) + (1 - g(l)) \int_0^a \left(1 - H\left(\frac{l}{a - \tau}\right)\right) \kappa(\tau) d\tau$$

where

$$g(l) = \int_0^{\infty} h(r) \int_{l/r}^{\infty} \int_{l/r}^{v} \frac{s - l/r}{v - l/r} f_S(s) f_T(v - s) ds dv dr$$

and

$$\kappa(a) = \int_a^{\infty} \frac{f_T(x)}{x} dx.$$

Differentiating with respect to a, we find:

$$\lambda(l, a) = g(l) \frac{l}{a^2} h\left(\frac{l}{a}\right) + (1 - g(l)) \int_0^a \frac{l}{(a - \tau)^2} \kappa(\tau) h\left(\frac{l}{a - \tau}\right) d\tau.$$

UU IR Author Manuscript
UU IR Author Manuscript

University of Utah Institutional Repository
Author Manuscript

1.2 Estimation of input signal from body signal

The isotope composition of the j^{th} pool contributing to hair formation at time t is $\delta_j^t = \delta_j^{t-1} e^{-\lambda_j \Delta t} + \delta^{eq}(1 - e^{-\lambda_j \Delta t})$ where δ_j^{t-1} is the isotope composition of the j^{th} pool at time $t-1$, Δt is the difference in time between $t-1$ and t, λ_j is the rate constant of the j^{th} pool, and δ_{eq} is the isotope composition of the pool if it were at instantaneous equilibrium with the environment. For a p pool system, δ_{eq} can be calculated incrementally from the stable isotope signal of a single hair, δ_H^t, as $\delta_{eq}^t = \frac{\delta_H^t - \sum_{i=1}^{p} f_i \delta_i^{t-1} e^{-\lambda_i \Delta t}}{\sum_{i=1}^{p} f_i (1 - e^{-\lambda_i \Delta t})}$ where f_i is the fractional contribution of of pool i to the pool at equilibrium with hair.

UU IR Author Manuscript
UU IR Author Manuscript

INSTITUTIONAL REPOSITORY
THE UNIVERSITY OF UTAH
University of Utah Institutional Repository
Author Manuscript

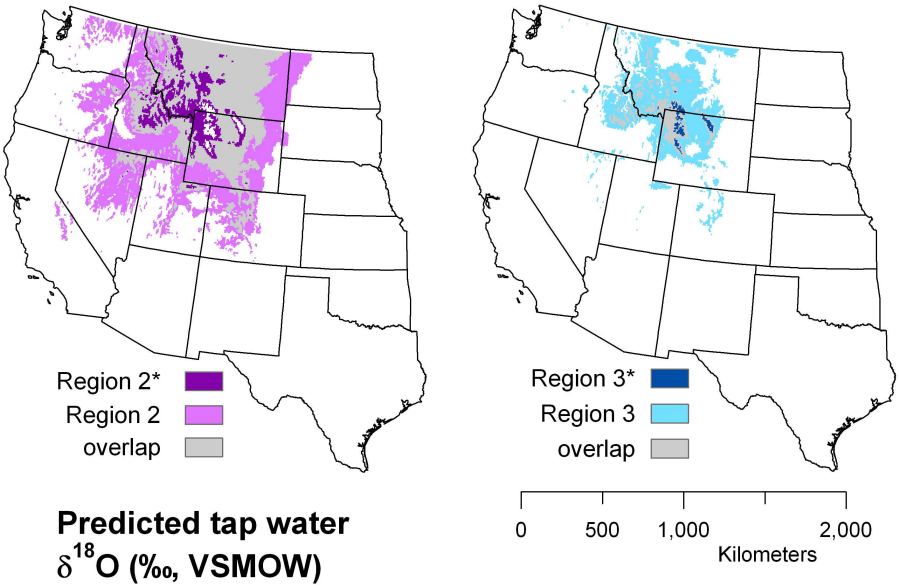

Figure S1: Comparison of Region 2 with Region 2* and Region 3 with Region 3*.

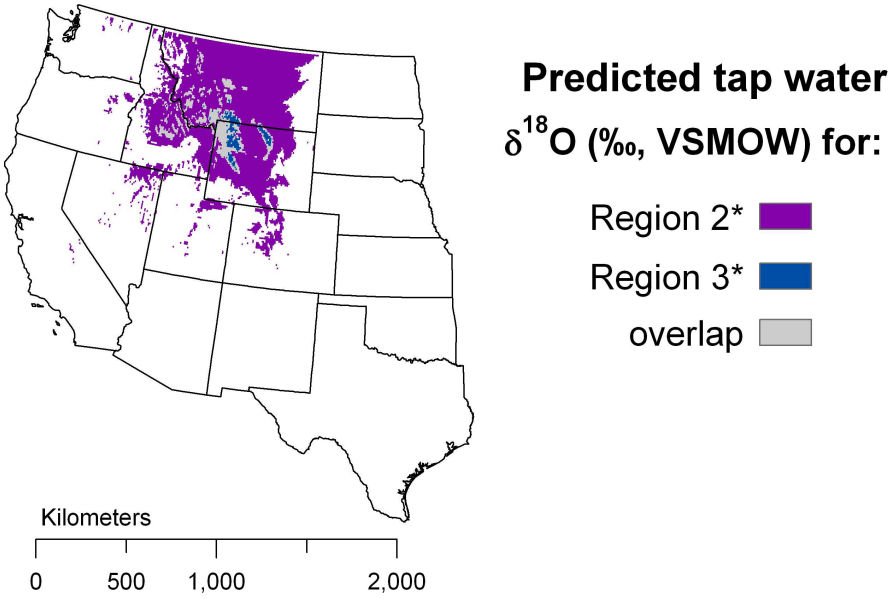

Figure S2: Comparison of Region 2* with Region 3*.

UU IR Author Manuscript
UU IR Author Manuscript

University of Utah Institutional Repository
Author Manuscript

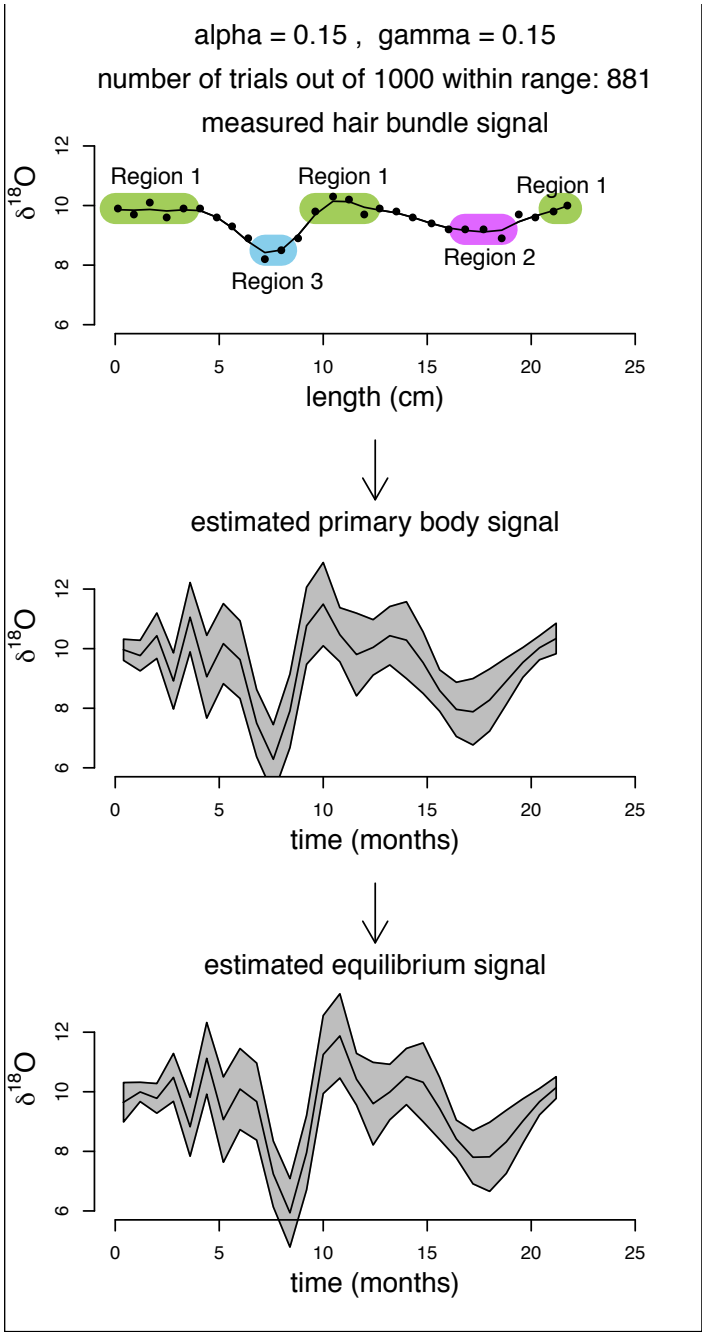

Figure S3: Murder victim inversion with $\alpha = 0.15$ and $\gamma = 0.15$.

UU IR Author Manuscript
UU IR Author Manuscript

University of Utah Institutional Repository
Author Manuscript

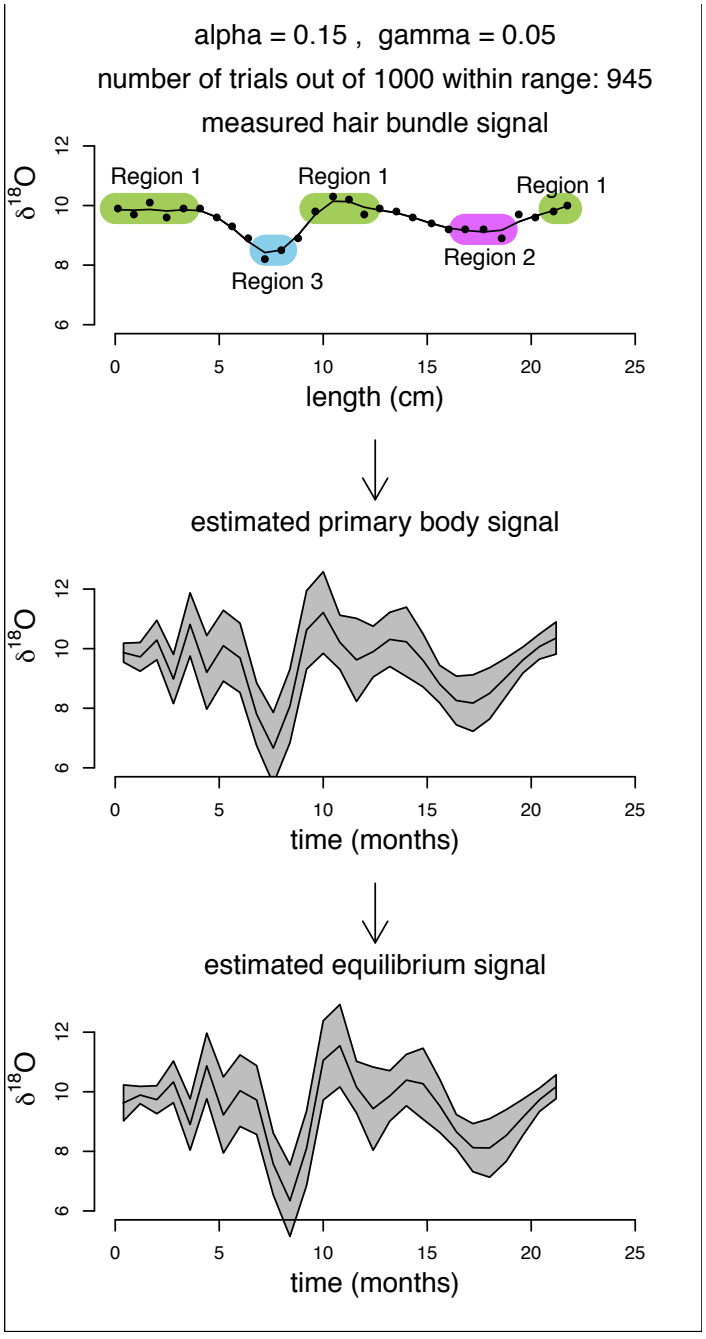

Figure S4: Murder victim inversion with $\alpha = 0.15$ and $\gamma = 0.05$.

UU IR Author Manuscript
UU IR Author Manuscript

University of Utah Institutional Repository
Author Manuscript

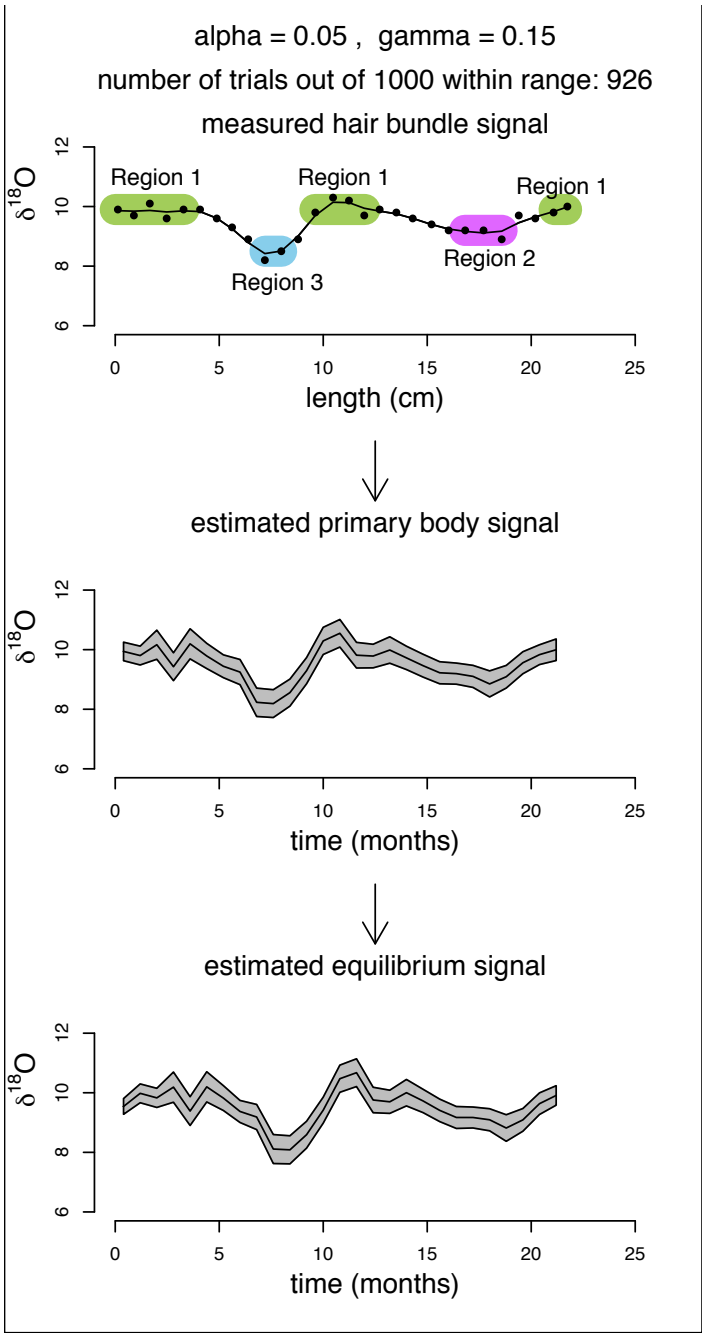

Figure S5: Murder victim inversion with $\alpha = 0.05$ and $\gamma = 0.15$.

UU IR Author Manuscript
UU IR Author Manuscript

University of Utah Institutional Repository
Author Manuscript

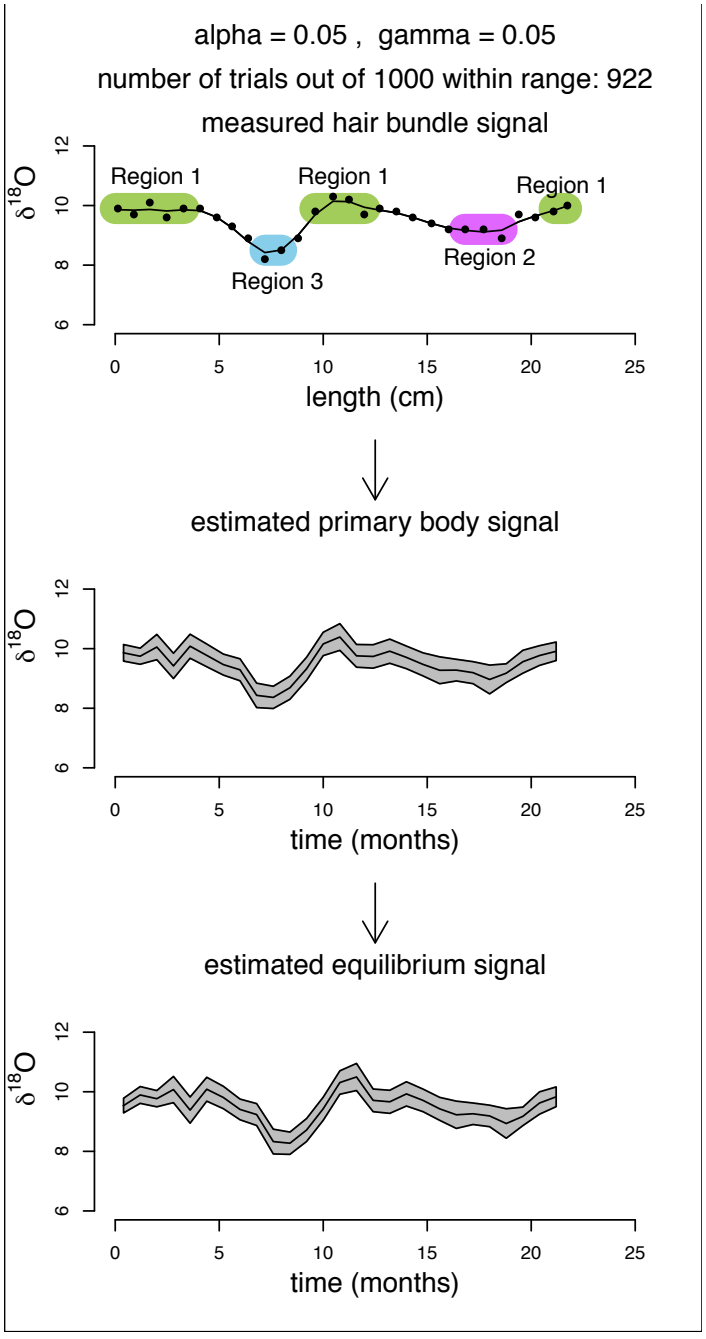

Figure S6: Murder victim inversion with $\alpha = 0.05$ and $\gamma = 0.05$.

UU IR Author Manuscript
UU IR Author Manuscript